FEBS Letters 535 (2003) 34–38 FEBS 26895

The p7 protein of hepatitis C virus forms an ion channel that is blocked by the antiviral drug, Amantadine

Stephen D.C. Griffin[a], Lucy P. Beales[a], Dean S. Clarke[a], Oliver Worsfold[b], Stephen D. Evans[c], Joachim Jaeger[a], Mark P.G. Harris[a], David J. Rowlands[a,*]

[a] *School of Biochemistry and Molecular Biology, University of Leeds, Division of Microbiology Old Medical School, Thoresby Place, Leeds LS2 9JT, UK*
[b] *Fujirebio Inc., 51 Komiya-cho, Hachioji-shi, Tokyo 192-0031, Japan*
[c] *Department of Physics, University of Leeds, Leeds LS2 9JT, UK*

Received 4 November 2002; accepted 27 November 2002

First published online 23 December 2002

Edited by Hans-Dieter Klenk

Abstract Hepatitis C virus (HCV) cannot be grown in vitro, making biochemical identification of new drug targets especially important. HCV p7 is a small hydrophobic protein of unknown function, yet necessary for particle infectivity in related viruses [Harada, T. et al., (2000) J. Virol. 74, 9498–9506]. We show that p7 can be cross-linked in vivo as hexamers. *Escherichia coli* expressed p7 fusion proteins also form hexamers in vitro. These and HIS-tagged p7 function as calcium ion channels in black lipid membranes. This activity is abrogated by Amantadine, a compound that inhibits ion channels of influenza [Hay, A.J. et al. (1985) EMBO J. 4, 3021–3024; Duff, K.C. and Ashley, R.H. (1992) Virology 190, 485–489] and has recently been shown to be active in combination with current HCV therapies.

Key words: Hepatitis C virus; Flavivirus; p7; Viroporin; Amantadine; Antiviral therapy

1. Introduction

Hepatitis C virus (HCV) is a major cause of chronic hepatitis, cirrhosis and hepatocellular carcinoma [4] and is now the leading indication for liver replacement surgery in the developed world. Most infections result in a chronic carrier state and current therapies are expensive, poorly tolerated and effective in only 50% of cases. Of particular concern is the emergence of viral resistance to these regimes [5,6].

HCV belongs to the *Hepacivirinae* genus of the family Flaviviridae [7]. The RNA genome is translated into a single polyprotein, which is proteolytically processed [8]. The functions of several of the viral proteins are poorly understood and study of the virus is complicated by the inability to culture it in vitro. p7 is a small hydrophobic protein located between the structural and non-structural regions of the polyprotein [9,10]. It is predicted to comprise two membrane-spanning helices linked by a small charged loop, and recent studies have confirmed that it is indeed membrane associated and mostly located in the endoplasmic reticulum [11]. Characteristics of p7 are reminiscent of a group of proteins known as viroporins. These homo-oligomerise to form ion channels and are frequently involved in virus assembly and/or release [12–18]. Disruption of viroporin function frequently abrogates viral infectivity, rendering them suitable targets for antiviral drug development.

2. Materials and methods

2.1. Generation of p7 expression constructs

The p7 sequence from the J4 infectious clone of HCV genotype 1B [19] was amplified by polymerase chain reaction (PCR) using a proofreading polymerase (Vent, New England Biolabs) with specific primers and introduced into the mammalian expression vector pCDNA3.1 (Invitrogen) giving the construct pCDNAp7, or the bacterial glutathione-S-transferase (GST) fusion vector pGEX4T1 (Amersham Pharmacia Biotech) to give pGEXp7. A 6-HIS tag was incorporated into the forward primer to generate a HIS-p7 cassette, used to generate pGEXHp7.

2.2. Protein cross-linking assay

HepG2 cells (2×10^5) were transfected by the BBS calcium phosphate method with 2 μg pCDNAp7 or control vector. 48 h post-transfection, cells were washed, scraped into phosphate-buffered saline (PBS) and split into two separate tubes, to one of which DSP (dithio-bis-succinimidyl proprionate, Pierce Endogen) was added to 1 mM final concentration and incubated at room temperature for 30 min. The reaction was quenched with 10 mM Tris–Cl pH 7.5, and the cells lysed and subjected to non-reducing sodium dodecyl sulphate–polyacrylamide gel electrophoresis (SDS–PAGE) with the exception of one cross-linked sample that was adjusted to 100 mM dithiothreitol (DTT). p7 was subsequently detected by immunoblot using a mouse polyclonal antiserum raised against a peptide corresponding to the N-terminal 13 residues of p7. For cross-linking of purified HIS-p7 (see below), 3 μg of protein in PBS in the presence of unilamellar lipid vesicles was incubated with DSP as above. Immunoblotting was performed using a sheep polyclonal antiserum raised against purified bacterially expressed GST-HIS-p7.

2.3. Transmission electron microscopy

50 ng protein was added to PBS in the presence or absence of artificially synthesised unilamellar vesicles or microsomal membranes (Promega, UK) in a volume of 125 μl. For immunogold labelling, a molar equivalent of biotinylated anti-GST monoclonal antibody (Serotech) was added along with a three-fold molar excess of streptavidin-coated 10 nM gold particles (Sigma). Samples were prepared by the Valentine technique. Briefly, the diluted sample was adsorbed to carbon film for 30 s. The carbon was then washed in water and negatively stained for 1 min in 2% uranyl acetate and mounted onto gold-plated copper grids. Electron micrographs were taken on a Phillips CM10 microscope.

2.4. Expression and purification of protein from Escherichia coli

Expression of GST fusions was induced in the presence of 0.1 mM IPTG (isopropyl β-D-thiogalactopyranoside) in *E. coli* DH5α. Protein

*Corresponding author. Fax: (44)-113-3435638.
E-mail address: djrowlands@bmb.leeds.ac.uk (D.J. Rowlands).

0014-5793/02/$22.00
doi:10.1016/S0014-5793(02)03851-6

was purified according to standard methods [20] and dialysed against PBS (or methanol where appropriate for use in calcium-containing electrolyte). HIS-p7 was generated by overnight cleavage with thrombin at 10 units/mg of fusion protein and separated by GSTrap™ (Amersham Pharmacia Biotech) chromatography followed by collection of the flow-through after passing through a 10 000 MWt filter (Microsep, Pall life sciences).

2.5. Ion channel formation in BLM

Equivalent molar amounts of fusion protein or derivatives were added to the *trans* chamber of a thoroughly cleaned BLM chamber containing a bilayer comprised of an equimolar mixture of phosphatidyl serine and phosphatidyl ethanolamine. The two Ag/AgCl electrodes were placed in a Faraday cage to minimise noise during current recordings and connected to a computer via an AXON patch-clamp filtered at 50 Hz, an ADC interface and a DAT recorder. AXON *pclamp* software was utilised to record and analyse the traces. To monitor the effect of Amantadine (Aldrich) on the formation of ion channels, 40 μl of Amantadine (20 μM in methanol) was added to both *cis* and *trans* compartments giving a final concentration of 1 μM. The current traces showing blocking of ion channels were recorded within 10 s after Amantadine injection. Traces shown are representative 10–15 s windows from over 10 min of readings obtained in each experiment. Each experiment was performed at least twice with different protein preparations.

3. Results

3.1. HCV p7 is able to homo-oligomerise in membranes

To determine whether p7 possesses the ability to oligomerise we expressed the protein in the hepatoma cell line, HepG2, and stabilised higher order assemblages in living cells using a lipid-soluble, cleavable cross-linking reagent, DSP. Total cellular protein was analysed and p7 detected by immunoblotting with an anti-p7 polyclonal antiserum (Fig. 1A, left-hand panel). In cross-linked samples a band migrating at 42 kDa was reproducibly observed which was absent from controls. Furthermore, the 42 kDa band was not seen in reducing conditions which cleaved DSP, indicating the presence of a hexameric form of p7 stabilised by the cross-linking reagent. Monomeric p7 from cell lysates transferred poorly, if at all, to the trapping membrane. In addition, HIS-p7 (see below) formed hexamers in vitro in the presence of DSP (Fig. 1A, right-hand panel) as well as dimers, suggesting that hexameric p7 assembles via an interaction between three such intermediates. The bands at 26 and 35 kDa represent trace contaminants of GST and GST-HIS-p7 respectively as assessed by blotting with an anti-GST antibody (data not shown).

High yields of p7 were obtained by expression as a GST fusion in *E. coli*. Fusion proteins or GST alone were examined by transmission electron microscopy (TEM) following negative staining with uranyl acetate in the presence or absence of lipids. GST-p7 formed ring structures at high frequency in the presence of lipid (Fig. 1B) and also sporadically in aqueous solution (data not shown). These structures were not observed in the absence of GST-p7, or in the presence of GST alone (data not shown), indicating that ring formation was solely due to the p7 component of the fusion protein. Immunogold labelling confirmed that the rings comprised GST moieties on the outside surrounding an electron dense core of approxi-

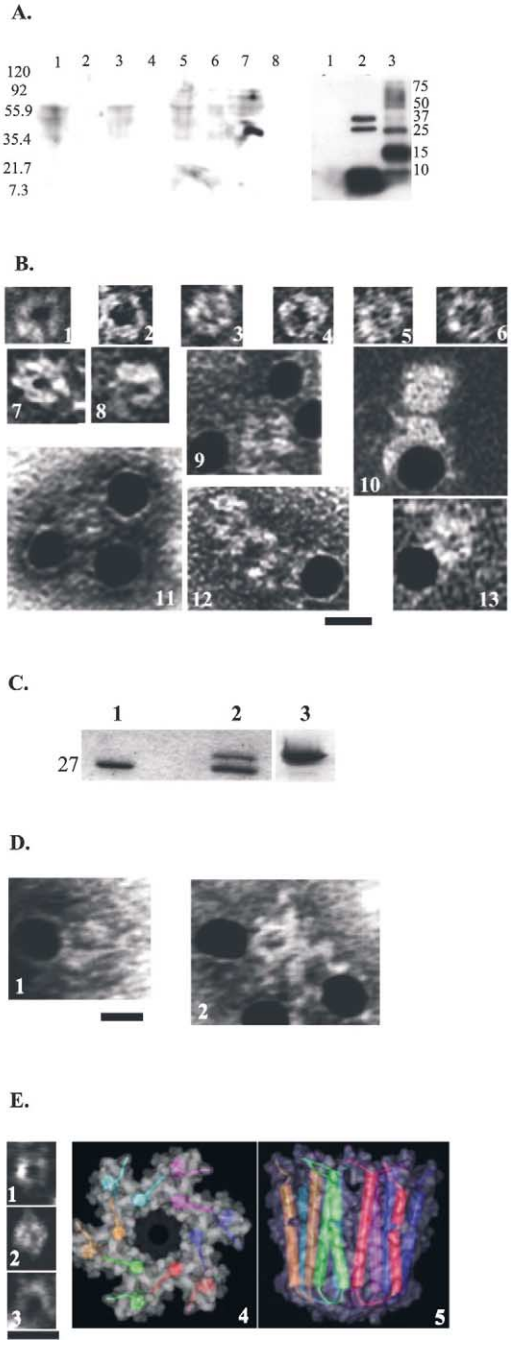

Fig. 1. Hexamerisation of HCV p7. A: Protein from transiently transfected HepG2 hepatoma cells or recombinant HIS-p7 was cross-linked using the compound DSP (Pierce Endogen) and immunoblotted with an anti-p7 polyclonal serum (see Section 2). Left-hand panel, lanes 1, mock transfected cells; 2, mock transfected cells+DSP; 3, pCDNA3.1 transfected cells (control vector); 4, pCDNA3.1 transfected cells+DSP; 5, pCDNAp7 transfected cells; 6, pCDNAp7 transfected cells+DTT; 7, pCDNAp7 transfected cells+DSP; 8, pCDNAp7 transfected cells+DSP+DTT. Right-hand panel, lanes 1, 3 μg bovine serum albumin (BSA); 2, 3 μg HIS-p7; 3, 3 μg HIS-p7+DSP. B: GST fusions of p7 analysed by TEM in the presence of microsomal membranes (panels 1–6) or artificially synthesised unilamellar vesicles (panels 7–13). Panels 9–13 show protein immunolabelled with 10 nm gold particles. Scale bar represents 10 nm. C: SDS–PAGE of purified GST fusion proteins showing stabilisation following introduction of 6-HIS linker between GST and p7 components of fusion proteins. Lanes 1, GST; 2, GST-p7; 3, GST-HIS-p7. D: TEM of GST-HIS-p7 with immunogold labelling. Scale bar represents 10 nm. E: Panels 1–3, TEM of ring structures obtained when cleaved HIS-p7 incubated with unilamellar vesicles. Scale bar represents 5 nm. Panels 4 and 5 show planar and side-on view of predicted p7 hexamer space-filling models, generated using the ONO 6.2.2 programme.

mately 4 nm diameter, the entire structure being 10 nm across. The structures contained six subunits in each ring, consistent with cross-linking studies.

Greatly improved yield and stability of the GST fusion protein was achieved by introducing a 6-histidine tag into the polylinker to produce GST-HIS-p7 (Fig. 1C). This fusion product again formed 10 nm ring structures in the presence of lipids (Fig. 1D) which were also immunogold labelled. Furthermore, thrombin-induced cleavage to release the HIS-p7 portion of the fusion protein allowed generation of a near-native p7 that also formed ring structures by TEM in the presence of lipid (Fig. 1E) of 3–5 nm diameter. Computer modelling was used to assess the likely stability and structure of the p7 hexamer. The amino acids of p7 were mapped onto a backbone of two α-helical domains of bacteriorhodopsin and the orientation of each individual side chain modelled by comparison with a database of protein crystal structures. This allowed p7 amino acid side chains to be oriented relative to neighbouring residues by assessing consensus bond rotations and stoichiometric constraints (ONO 6.2.2 programme). The predicted structure is a channel of 2.3 nm diameter comprising the amphipathic N-terminal helices of p7 forming a channel, stabilised by the C-terminal helices interacting with an adjacent p7s′ N-terminal helix (Fig. 1E). The entire predicted structure measures 5.4 nm in diameter, consistent with TEM studies. The side chains of the charged loop are predicted to project into the channel, likely forming a gate component. This may explain why mutations of this region alone in the related pestivirus bovine viral diarrhoea virus (BVDV) are sufficient to abrogate infectivity [1].

3.2. HCV p7 forms ion channels in artificial membranes

The ability of GST-p7 and derivatives to form ion channels in vitro was investigated using a black lipid membrane conductivity system in which ion channel activity is measured as a flow of current across an otherwise insulating membrane. Representative traces from BLM experiments are shown. In the absence of protein (Fig. 2A, top panel) negligible current was observed indicating that the bilayer was intact; bilayer formation itself was confirmed by capacitance measurements. The addition of GST did not change the permeability of the bilayer to potassium ions (Fig. 2A, middle panel). When GST-p7 was added, however, transient current spikes were observed (Fig. 2A, bottom panel), indicating that GST-p7 formed short-lived channels. Channel formation was voltage dependent and no current flowed in the presence of protein for *trans*-membrane voltages lower than −120 mV (data not shown). Furthermore, the ion current was directional (data not shown), suggesting that GST-p7 inserted into the membrane in a single orientation.

GST-HIS-p7 formed more efficient ion channels than GST-p7, both in frequency of channel opening and the amount of current that flowed (Fig. 2B). As with GST-p7, the flow of current appeared to be directional (data not shown). Furthermore, GST-HIS-p7 displayed ion selectivity, for Ca^{2+} over K^+, as evidenced by greater burst activity and increased amplitude (Fig. 2C).

Cleaved HIS-p7 was used to examine the ion channel activity of p7 in the absence of a fusion protein partner. This greatly increased channel activity (Fig. 3B) compared to the parental GST-HIS-p7, indicating that the fusion partner had been impeding ion channel formation. In accordance with this

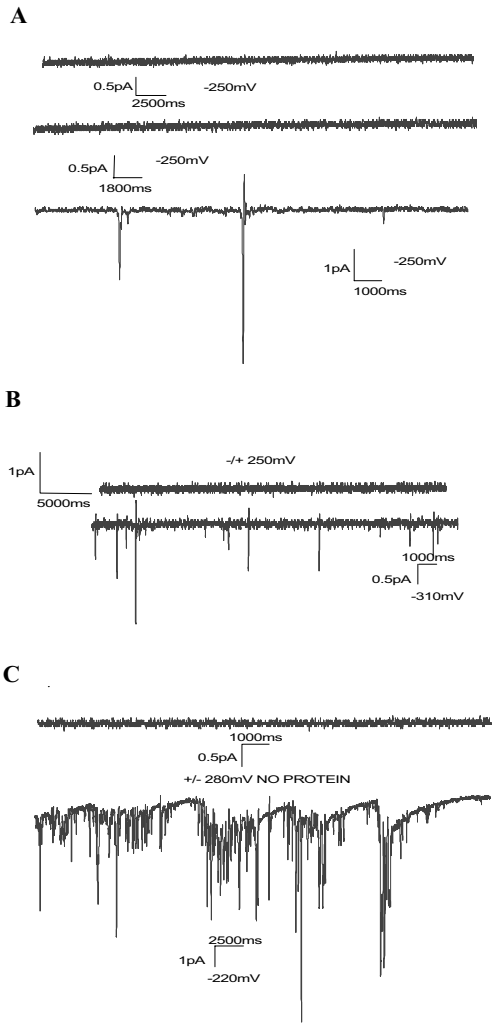

Fig. 2. Ion channel activity of GST fusions in black lipid membrane systems. A: Ion channel activity of GST-p7. Top panel shows current flow across membrane bilayer in the absence of protein. Middle panel shows trace obtained after the addition of GST. Bottom trace shows burst activity obtained after the addition of GST-p7 to the same chamber. B: Ion channel formation by GST-HIS-p7. Top trace shows baseline in the absence of protein and bottom trace shows current flow upon addition of GST-HIS-p7. C: Ion channel formation by GST-HIS-p7 with calcium-containing electrolyte (0.1 M $CaCl_2$) in place of potassium. Top trace shows baseline current in the absence of protein and bottom trace shows burst activity upon addition of GST-HIS-p7. Scales for time (horizontal axis) and current (vertical axis) are shown for each trace.

observation, the *trans*-membrane voltage necessary to induce channel formation by HIS-p7 was as little as −15 mV (data not shown), though voltages were kept to a similar range for consistency between experiments. In contrast to the GST fusion proteins, with HIS-p7 the ion transport displayed no directional dependence suggesting that it either inserted into the membrane in both orientations, or that the channel itself showed no directional dependence. HIS-p7 displayed an even greater preference for Ca^{2+} than did GST-HIS-p7 (Fig. 3C).

3.3. HCV p7 ion channel formation is inhibited by Amantadine

Amantadine has been used clinically to treat influenza A infection [21] and acts by inhibiting the M2 ion channel encoded by the virus [2,3,22–24]. As HIS-p7 had been shown in this study to efficiently form ion channels in a system very

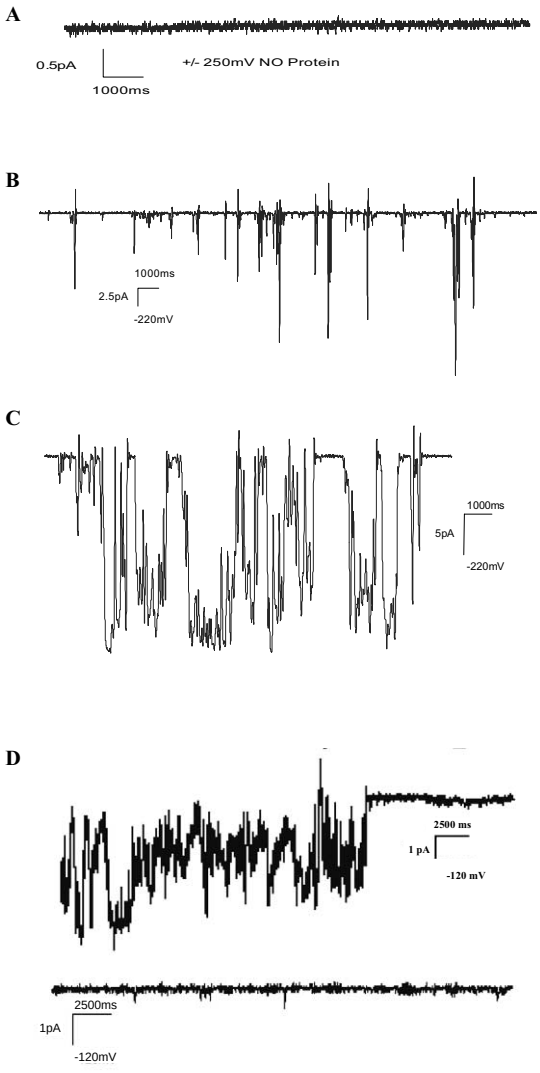

Fig. 3. Ion channel activity of HIS-p7 and the effect of Amantadine. A: Representative trace showing baseline current in the absence of added protein. B: Trace of burst activity following addition of HIS-p7 to system containing potassium electrolyte (0.1 M KCl). C: Trace of burst activity following addition of HIS-p7 in calcium-containing electrolyte (0.1 M $CaCl_2$). D: Effect of Amantadine on HIS-p7 ion channel formation. Top trace showing burst activity of HIS-p7 under standard conditions. Bottom trace showing activity approximately 10 s following the introduction of Amantadine to a final concentration of 1 μM to both *cis* and *trans* chambers. Burst activity was absent for the remainder of the assay following Amantadine injection. Scales for time (horizontal axis) and current (vertical axis) are shown for each trace.

similar to that used to characterise M2 [3], we investigated the effect of Amantadine on p7 channel formation. Amantadine was added to a final concentration of 1 μM; a concentration previously shown to specifically inhibit M2 in vitro [3]. The high-efficiency channel opening of HIS-p7 was abrogated by the drug at this concentration (Fig. 3D). This effect was specific to the near-native HIS-p7 as GST-HIS-p7 was not affected by the addition of Amantadine, even at concentrations of 1 mM (data not shown).

4. Discussion

This is the first demonstration of a function for the p7 protein of HCV as a viral ion channel, most likely responsible for the flow of calcium ions from the endoplasmic reticulum into the cytoplasm as has been observed for other viroporins [14,16]. The equivalent protein of the related pestivirus, BVDV, has been shown to be essential for the formation of infectious virus particles [1], and taken together with the functions of other viroporins, it is likely that HCV p7 acts at a similar point in the virus life-cycle. Unfortunately, the current lack of a HCV culture system that efficiently produces infectious virus particles prevents this hypothesis from being tested and the effect of Amantadine on viral replication in culture is unknown, though Amantadine has been shown to inhibit viral replication in patient PBMC cultured ex vivo [25]. In addition, Amantadine has been used in clinical trials on HCV-infected individuals and shows a significant degree of efficacy, often improving current therapeutic regimes comprising interferon α and ribavirin [26–29]. Amantadine has been shown not to affect the functions of HCV protease, helicase, ATPase, polymerase, or internal ribosome entry in biochemical assays [30]. We propose that the effects of Amantadine in such studies are, therefore, due to inhibition of p7 function, making the search for other p7 ion channel blocking compounds an attractive new approach to anti-HCV chemotherapy.

Acknowledgements: We thank Helen Pearce for generating the mouse anti-p7 polyclonal serum and Caitriona Dennis for advice on protein purification. This work was funded by the Medical Research Council, UK.

References

[1] Harada, T., Tautz, N. and Thiel, H.J. (2000) J. Virol. 74, 9498–9506.
[2] Hay, A.J., Wolstenholme, A.J., Skehel, J.J. and Smith, M.H. (1985) EMBO J. 4, 3021–3024.
[3] Duff, K.C. and Ashley, R.H. (1992) Virology 190, 485–489.
[4] Choo, Q.L., Kuo, G., Weiner, A., Wang, K.S., Overby, L., Bradley, D. and Houghton, M. (1992) Semin. Liver Dis. 12, 279–288.
[5] Enomoto, N. et al. (1996) N. Engl. J. Med. 334, 77–81.
[6] Chemello, L. et al. (1995) J. Viral Hepat. 2, 91–96.
[7] Robertson, B. et al. (1998) Arch. Virol. 143, 2493–2503.
[8] Clarke, B. (1997) J. Gen. Virol. 78 ((Pt 10)), 2397–2410.
[9] Selby, M.J., Glazer, E., Masiarz, F. and Houghton, M. (1994) Virology 204, 114–122.
[10] Lin, C., Lindenbach, B.D., Pragai, B.M., McCourt, D.W. and Rice, C.M. (1994) J. Virol. 68, 5063–5073.
[11] Carrere-Kremer, S., Montpellier-Pala, C., Cocquerel, L., Wychowski, C., Penin, F. and Dubuisson, J. (2002) J. Virol. 76, 3720–3730.
[12] Ewart, G.D., Sutherland, T., Gage, P.W. and Cox, G.B. (1996) J. Virol. 70, 7108–7115.
[13] Bodelon, G., Labrada, L., Martinez-Costas, J. and Benavente, J. (2002) J. Biol. Chem. 277, 17789–17796.
[14] Tian, P., Estes, M.K., Hu, Y., Ball, J.M., Zeng, C.Q. and Schilling, W.P. (1995) J. Virol. 69, 5763–5772.
[15] Aldabe, R., Barco, A. and Carrasco, L. (1996) J. Biol. Chem. 271, 23134–23137.
[16] van Kuppeveld, F.J., Hoenderop, J.G., Smeets, R.L., Willems, P.H., Dijkman, H.B., Galama, J.M. and Melchers, W.J. (1997) EMBO J. 16, 3519–3532.
[17] Pinto, L.H., Holsinger, L.J. and Lamb, R.A. (1992) Cell 69, 517–528.
[18] Betakova, T., Nermut, M.V. and Hay, A.J. (1996) J. Gen. Virol. 77 ((Pt 11)), 2689–2694.
[19] Yanagi, M., St Claire, M., Shapiro, M., Emerson, S.U., Purcell, R.H. and Bukh, J. (1998) Virology 244, 161–172.
[20] Smith, D.B. and Johnson, K.S. (1988) Gene 67, 31–40.
[21] Fleming, D.M. (2001) Int. J. Clin. Pract. 55, 189–195.
[22] Wang, C., Takeuchi, K., Pinto, L.H. and Lamb, R.A. (1993) J. Virol. 67, 5585–5594.

[23] Wang, C., Lamb, R.A. and Pinto, L.H. (1995) Biophys. J. 69, 1363–1371.
[24] Okada, A., Miura, T. and Takeuchi, H. (2001) Biochemistry 40, 6053–6060.
[25] Martin, J., Navas, S., Fernandez, M., Rico, M., Pardo, M., Quiroga, J.A., Zahm, F. and Carreno, V. (1999) Antiviral Res. 42, 59–70.
[26] Zilly, M., Lingenauber, C., Desch, S., Vath, T., Klinker, H. and Langmann, P. (2002) Eur. J. Med. Res. 7, 149–154.
[27] Torre, F., Giusto, R., Grasso, A., Brizzolara, R., Campo, N., Sinelli, N., Balestra, V. and Picciotto, A. (2001) J. Med. Virol. 64, 455–459.
[28] Brillanti, S., Levantesi, F., Masi, L., Foli, M. and Bolondi, L. (2000) Hepatology 32, 630–634.
[29] Smith, J.P. (1997) Dig. Dis. Sci. 42, 1681–1687.
[30] Jubin, R., Murray, M.G., Howe, A.Y., Butkiewicz, N., Hong, Z. and Lau, J.Y. (2000) J. Infect. Dis. 181, 331–334.